International Journal of GEOMATE, May, 2016, Vol. 10, Issue 21, pp. 1869-1876
Geotec., Const. Mat. & Env., ISSN: 2186-2982(Print), 2186-2990(Online), Japan

LOAD-STRAIN-TIME BEHAVOURS OF TWO POLYMER GEOGRIDS AFFECTED BY TEMPERATURE

Thitapan Chantachot[1], Warat Kongkitkul[2] and Fumio Tatsuoka [3]

[1,2]Faculty of Engineering, King Mongkut's University of Technology Thonburi, Thailand;
[3]Faculty of Science and Technology, Tokyo University of Science, Japan

ABSTRACT: A special series of tensile loading tests was performed on two types of geogrid using a wide variety of load and temperature histories to evaluate the effects of ambient temperature on their load-strain-time behaviours. The applied loading schemes included monotonic loading and sustained loading under different controlled ambient temperature conditions. The followings were found from test results and their analysis performed in this study. With an increase in the ambient temperature, the rupture strength and stiffness decreased while the creep strain increased associated with a decrease in the stiffness. The creep strain by sustained loading during which the temperature was elevated from 30 ^{o}C to 50 ^{o}C was significantly larger than the one by sustained loading during otherwise monotonic loading at the constant temperature equal to either 30 ^{o}C or 50 ^{o}C. The elastic stiffness decreased with an increase in the temperature while increased with the tensile load level. Importantly, the residual tensile strength observed at the same ambient temperature was essentially independent of pre-rupture loading histories.

Keywords: Geogrid, Temperature, Tensile loading test, Creep, Residual strength

1. INTRODUCTION

The effects of ambient temperature on the strength and stiffness of geosynthetic reinforcement is one of the important factors to be taken into account in the design of geosynthetic-reinforced soil (GRS) structures. Moreover, to prevent long-term creep rupture of geosynthetic reinforcement, allowable tensile strength of geosynthetic reinforcement is used in the design, as suggested by Koerner and GRI Standard Practice [1]-[3]. The allowable tensile strength is obtained by reducing the tensile rupture strength by fast loading tests using a creep reduction factor, which is typically between 1.5 to 4.0, depending on the type of geosynthetic and application [1]-[3].

The creep reduction factor is evaluated from a creep rupture curve formulated by analysing results originally from a set of conventional creep tests. However, this type of tests is extremely time-consumption, therefore extremely costly. To shorten the time required for the entire test program, the creep tests are often conducted at elevated temperatures in order to accelerate the creep process. In the method called the time-temperature superposition (TTS), a set of creep tests are performed on geosynthetics specimens until rupture at a set of constant but different ambient temperatures. The TTS can expedite the creep, but it requires multiple replicated specimens to obtain a reliable result. Then, the stepped isothermal method (SIM) was developed in order to avoid the effect of variance among the multiple specimens [4], in which the creep test is performed at a series of elevated constant temperatures on a single geosynthetic specimen.

To understand the load-deformation behaviour during creep of geosynthetics affected by temperature, a number of temperature-accelerated creep tests on geosynthetic reinforcements have been performed [5]-[8]. However, in these tests, only load-deformation responses during sustained loading are evaluated, whereas the behaviour after monotonic loading is restarted following sustained loading is not evaluated. Moreover, experiments to evaluate the effects of temperature on the tensile strength are limited. The study to evaluate the combined effects of sustained loading and temperature changes cannot be found in the literature.

In view of the above, in this study, a series of tensile loading tests were performed on two types of geogrid. Various loading schemes and temperature changes were applied to evaluate the effects of load and temperature histories on the load-deformation behaviour and rupture tensile strength.

2. APPARATUSES AND MATERIALS

2.1 Loading and Heating Apparatuses

A tensile loading test on a geogrid specimen was performed by using a load-controlled loading system [9]. The tensile load was applied by controlling the air pressure in the air cylinder. The loading direction (load/unload) and load rate were controlled by means of an electro-pneumatic transducer (EP).

The temperature surrounding the specimen was controlled by using a heating unit connected to a temperature-controlled chamber containing a test specimen (Fig. 1(a)). The heating unit consists of a heater, a network of air-pipes and a temperature controller. The heater provided hot air to the chamber via the air-pipes. By using this apparatus, the temperature inside the chamber can be controlled as planned [10].

2.2 Measuring Devices

A load cell was connected to the loading piston to measure the tensile load (Fig. 1(a)). A displacement sensor (Fig. 1(b)) was arranged on a tiny frame that was attached on the central part of the specimen to sensitively measure the local tensile deformation of the specimen. The ambient temperature surrounding the specimen was measured by using a thermo-couple that was installed inside the temperature-controlled chamber.

2.3 Test Materials

Two different polymer geogrids were used (Fig. 2): i) high-density polyethylene (HDPE); and ii) polypropylene (PP). HDPE geogrid is a uniaxial type designed for use as reinforcement in one direction. The aperture shape is long-elliptical. On the other hand, PP geogrid is a biaxial type. The size of aperture is 35 mm (centre-to-centre) in both longitudinal and transverse directions. The mechanical properties of these two geogrids according to their manufacturers are listed in Table 1.

3. TEST METHOD

3.1 Specimen Preparation

The top and bottom ends of respective specimens were clamped by using a pair of gripping device connected to the loading piston. The roller-clamp of each gripping device consists of a steel cylinder with a groove made to grip the specimen with a steel rod. A sheet of sand paper was glued on the surface of the roller-clamp to avoid slippage of the specimen around the roller clamp during testing (Figs. 1(a) and 1(b)). Prior to the start of each tensile loading test, a very small preload of 20 N was applied to minimise the settling error of specimen.

3.2 Test Program

The following three different loading and temperature histories, shown in Fig. 3, were employed:

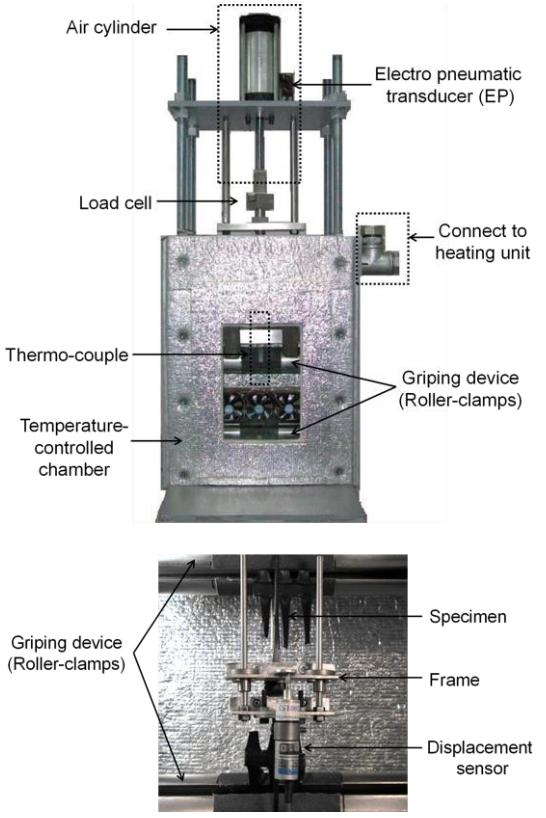

Fig. 1 (a) Tensile loading apparatus and measuring devices; and (b) installation of displacement sensor

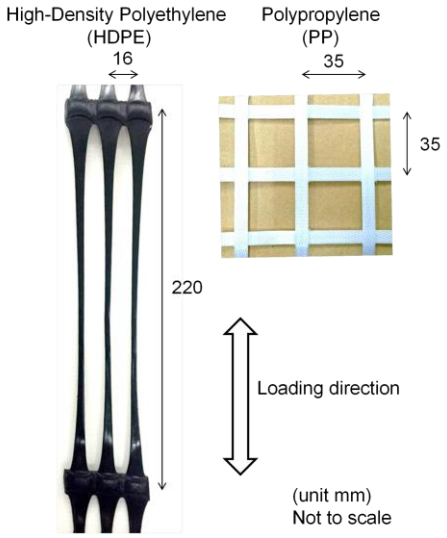

Fig. 2 Geosynthetic reinforcements

Table 1 Mechanical properties of geogrids

Type	Ultimate tensile strength (kN/m)	Yield point elongation (%)
HDPE	90	13
PP	≥ 40	≤ 8

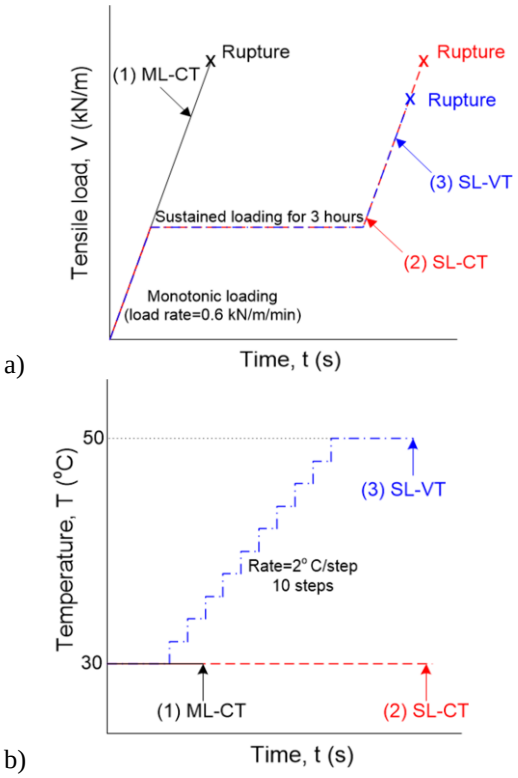

Fig. 3 Loading and temperature histories:
(1) ML-CT tests, performed at constant temperatures equal to 30 °, 35 °, 40 °, 45 ° or 50 °C.
(2) SL-CT tests, performed at constant temperatures equal to either 30 ° or 50 °C.
(3) SL-VT tests, performed increasing the temperature from 30 °C to 50 °C during sustained loading.
Remark: In this figure, only ML-CT and SL-CT tests at T=30 °C are depicted.

3.2.1 Monotonic loading-constant temperature (ML-CT)

Monotonic loading was performed at a constant load rate of 0.6 kN/m/min towards the specimen's rupture. The ambient temperature was kept constant between 30 °C and 50 °C throughout each test.

3.2.2 Sustained loading-constant temperature (SL-CT)

Monotonic loading was continued at a constant load rate of 0.6 kN/m/min until the tensile load became a certain value where sustained loading was performed for a period of three hours, followed by the restart of monotonic loading at the original load rate. The ambient temperature was controlled to be constant, either 30 °C or 50 °C, throughout each test.

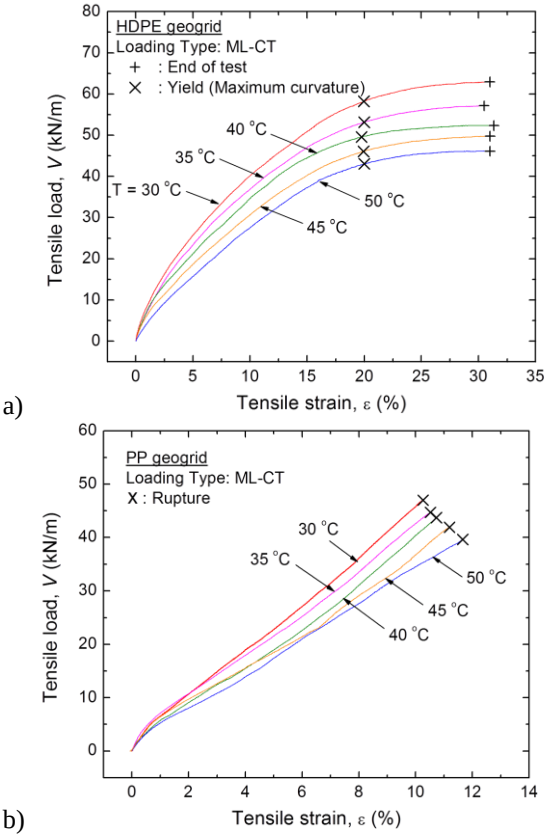

Fig. 4 Tensile load and strain relations from ML-CT tests: (a) HDPE; and (b) PP

3.2.3 Sustained loading-variant temperature (SL-VT)

This loading type is similar to SL-CT except that the temperature during sustained loading was increased from 30 °C to 50 °C in 10 steps at a rate of 2 °C/step.

4. TEST RESULTS AND DISCUSSIONS

4.1 Temperature Effects on Rupture Strength

Figs. 4(a) and 4(b) show the relationships between tensile load (V) and tensile strain (ε) from ML-CT tests on HDPE and PP geogrids, respectively. In these tests, HDPE geogrid did not reach the peak tensile load states at the largest strain applied, about 30 %. Hence, the rupture strength was defined by the yield load defined at the point of maximum curvature along the V-ε relation.

As the effects of strain rate on the tensile rupture strength (V_{max}) of geosynthetic reinforcement are significant [11], the measured values of V_{max} were corrected to the values at the same strain rate, 0.1 %/min (selected as a reference strain rate). As the loading apparatus used is of load-controlled type, the strain

Table 2 Test results from ML-CT loading type

Types	T (^{o} C)	$V_{max,cor}$ (kN/m)	ε_{rup} (%)	E_{50} (kN/m)
HDPE	30	53.1	19.98	481.3
	35	48.1	20.01	442.1
	40	44.9	19.75	401.0
	45	41.8	19.96	342.0
	50	39.1	20.00	292.2
PP	30	44.0	10.27	454.9
	35	43.2	10.52	428.7
	40	41.9	10.74	376.5
	45	40.5	11.20	358.3
	50	38.4	11.66	349.5

rate at rupture along different V-ε relations were different, controlled by the tangential stiffness at the moment of tensile rupture. The values of V_{max} at a strain rate of 0.1 %/min, $V_{max,cor}$, were obtained by correcting the measured values by numerical simulations based on the non-linear three-component model. In these simulations, it was assumed that the viscous property of the tested geogrids is of isotach type. The details of the correction are described in Kongkitkul et al. (2012) [10].

The values of $V_{max,cor}$ and rupture strain (ε_{rup}) are summarised in Table 2. The secant stiffness (E_{50}) of V-ε relation, defined as the ratio of 50% of V_{max} to ε at this point, is also listed in Table 2. Obviously, the values of $V_{max,cor}$ and E_{50} decrease significantly with an increase in the ambient temperature from 30 ^{o}C.

4.2 Creep Deformation Characteristics

The V-ε relations obtained from SL-CT tests at T = 30 ^{o}C and 50 ^{o}C are shown in Figs. 5 and 6, respectively. The V-ε relations from SL-VT tests are shown in Fig. 7. It may be seen from these figures that the V-ε curves before the start of sustained loading in SL-CT and SL-VT tests are nearly the same as those from ML-CT tests at the same temperature. This result indicates a high repeatability of test in this study.

The following trends of behaviour, as schematically illustrated in Fig. 8, are also seen:

1. In Fig. 7, in SL-VT tests, the V-ε curves immediately after the restart of monotonic loading at T = 50 ^{o}C, following sustained loading, are stiffer, while exhibiting larger strains, than those in ML-CT tests at T = 50 ^{o}C.
2. As seen by comparing Figs. 6 and 7, the V-ε curves immediately after the restart of monotonic loading at T = 50 ^{o}C in SL-VT tests are as stiff as those in SL-CT tests at T = 50 ^{o}C, although the strains are different.

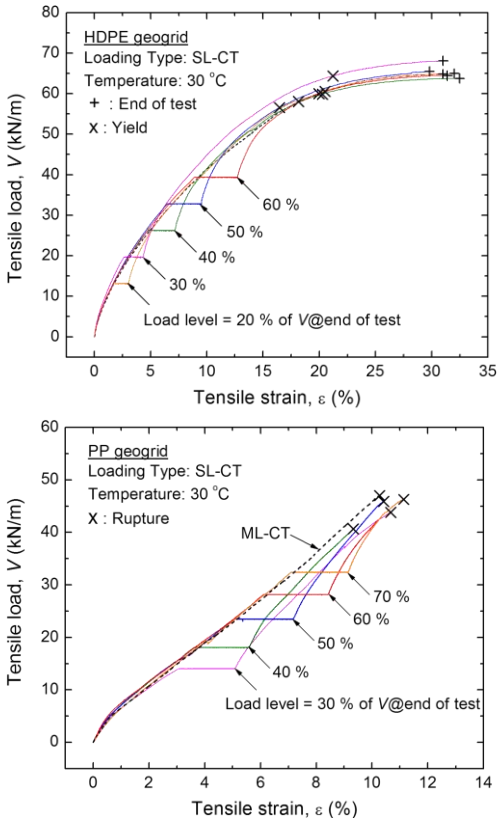

Fig. 5 Tensile load and strain relations at T = 30 ^{o}C from SL-CT tests: (a) HDPE; and (b) PP

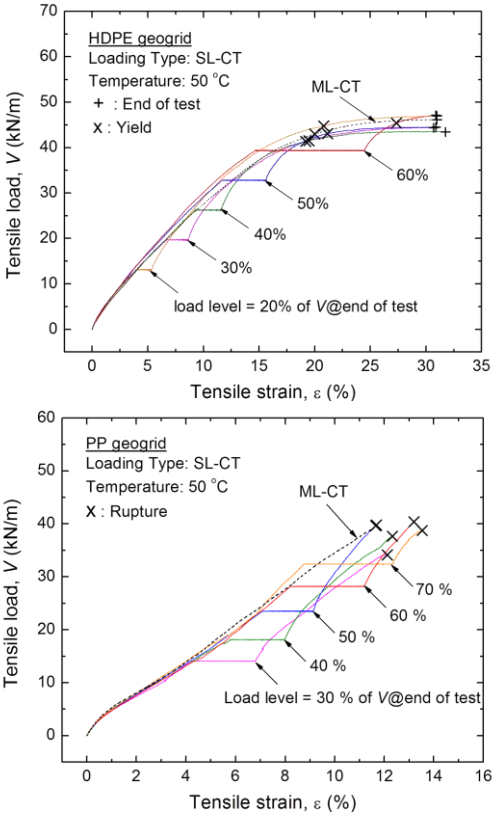

Fig. 6 Tensile load and strain relations at T = 50 ^{o}C from SL-CT tests: (a) HDPE; and (b) PP

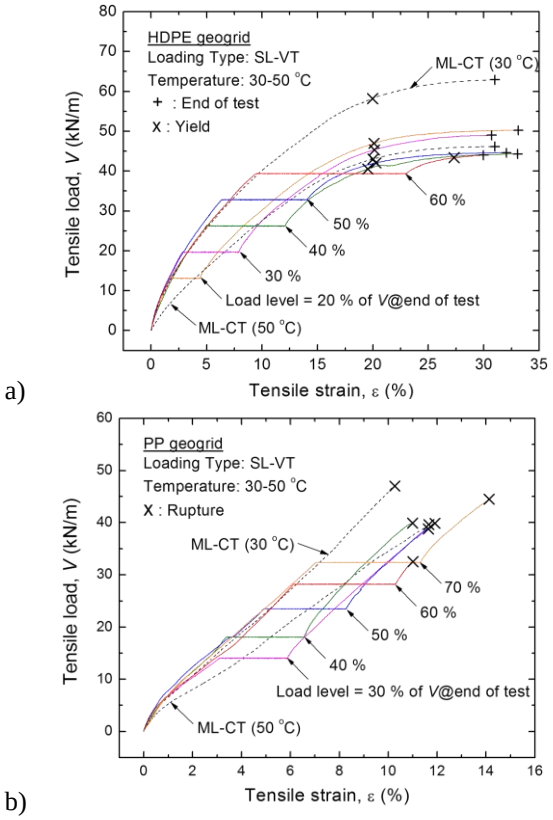

Fig. 7 Tensile load and strain relations from SL-VT tests: (a) HDPE; and (b) PP

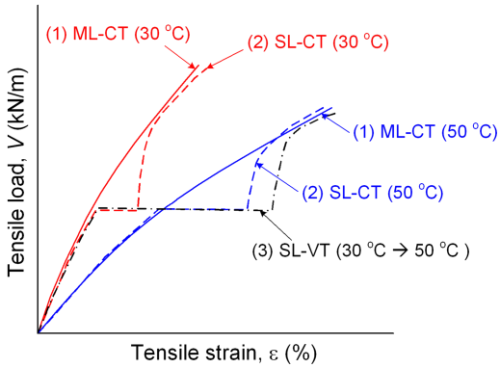

Fig. 8 Schematic diagram showing the trend of behaviour in SC-VT tests

3. The subsequent *V*-ε curves approaching the ultimate failure at T = 50 °C in SL-CT and SL-VT tests tend to re-joins those in ML-CT tests at T = 50 °C.
4. Reflecting the trends described above, the creep strain by sustained loading during which the temperature increased from 30 °C to 50 °C in SL-VT tests is significantly larger than the one in SL-CT at T = 30 °C or 50 °C.

4.3 Effects of Temperature on Creep Strain

Fig. 9 compares the creep strains (ε_{CR}) defined as the strain increment by sustained loading for a period of 3 hours at different load levels observed in SL-CT and SL-VT tests. These ε_{CR} values have been corrected to those when the initial creep strain rate is 0.1 %/min and 0.05 %/min for HDPE and PP geogrids, respectively. That is, in this study, the actual initial creep strain rate at the start of respective sustained loading stages was different due to different load levels and temperatures. On the other hand, the ε_{CR} for a given period decreases with a decrease in the initial creep strain rate and vice versa [11]. Therefore, to remove the effects of initial creep strain rate, the start of sustained loading was redefined at the moment when the strain rate was the same (0.1 %/min or 0.05 %/min). Then, the total creep strain for a period of three hours starting from the redefined initial state was obtained from the time history of creep strain obtained by extrapolating the measured time history (Fig. 10).

It may be seen from Fig. 9 that, in SL-CT tests at performed at different constant temperatures, the creep strain increased with an increase in the temperature, associated with a decrease in the stiffness (Table 2). Reference [13] showed that this trend of behaviour can be simulated by the non-linear three-component model taking into account the temperature effects.

It may also be seen from Fig. 9 that the creep strain increment by sustained loading during which the temperature increased from 30 °C to 50 °C in SL-VT tests is significantly larger than both of those at T = 30 °C and 50 °C in SL-CT tests. Besides, the creep strain increment in SL-VT tests is not a simple summation of those at T = 30 °C ° and 50 °C in SL-CT tests. This trend is due to the viscous property coupled with temperature effects in a non-linear manner affected by load-temperature history. In this respect, Figs. 11(a) and 11(b) show the time histories of creep strain rate ($d\varepsilon_{CR}/dt$) during sustained loading at the same load level in SL-CT and SL-VT tests of HDPE and PP geogrids. In these figures, the moments when the temperature were changed in the SL-VT case are marked "x". It may be seen that, as far as the load and temperature are kept constant in SL-CT tests, the creep strain rate consistently and smoothly decreased with time towards a value much lower than the initial value. On the other hand, in SL-VT tests, the relationship between the creep strain rate and the elapsed time exhibits a discontinuous decrease in the decreasing rate of creep strain rate at the moments when the temperature changed. Importantly, the creep strain

rate at the start of the last stage at 50 °C in SL-VT test and those during this stage are significantly higher than those in SL-CT test despite that the temperature is the same (50 °C) and the elapsed time is the same. This trend indicates that the instantaneous creep strain rate is not a unique function of current load, strain and temperature, but it is controlled by loading and temperature histories. It will be reported in the near future that these trends of behaviour can be simulated by the non-linear three-component model taking into account the temperature effects.

4.4 Effects of Temperature on Elastic Stiffness

Figs. 12(a) and 12(b) show full-log plots of the relationships between the equivalent elastic stiffness (k_{eq}) and the load level (V/V_{max}) obtained from SL-CT at T = 30 °C and 50 °C for HDPE and PP geogrids, respectively. The k_{eq} value was determined from the slope of the V-ε curves immediately after the restart of monotonic loading following sustained loading. The behaviour at this moment is highly linear-elastic, as described in Section 4.2. The respective relationships shown in Fig. 12 can be fitted by a linear relation. It can be readily seen that the k_{eq} value decreases with an increase in the temperature, while it increases with an increase in the load level [10].

4.5 Effects of Loading and Temperature History on Residual Rupture Strength

Figs. 13(a) and 13(b) show the residual tensile rupture strengths plotted against the temperature at the end of the respective tests (i.e., the temperature when the residual strength was measured) of HDPE and PP geogrids, respectively. The data from ML-CT tests at different constant temperatures are denoted by solid squares. The average relation is denoted by segmental lines connecting these data points. Two other lines shown above and below this central line denote the rupture strengths that are 90 % and 110 % of the average value at the same temperature. The other data points denote the residual strengths V_{max} defined at a strain rate of 0.1 %/min, $V_{max,cor}$, obtained by restarting monotonic loading following sustained loading in SL-CT and SL-VT tests. It may be seen that, under the same temperature at rupture and the same strain rate, the residual tensile strengths for the different pre-rupture loading and temperature histories examined in this study are similar. With PP geogrid, the scatter of data is relatively large. However, there is no systematic trend due to any specific pre-rupture loading/temperature history. Therefore, it can be concluded that the residual strength of the geogrids tested is a rather unique function of temperature and strain rate at rupture, while independent of pre-rupture loading/temperature history. That is, although the rising of ambient temperature exhibits negative effects on the load-deformation behaviour of geogrid, the residual strength is essentially a function of temperature at rupture, while creep by sustained loading is not a degrading phenomenon for the rupture strength of geogrid.

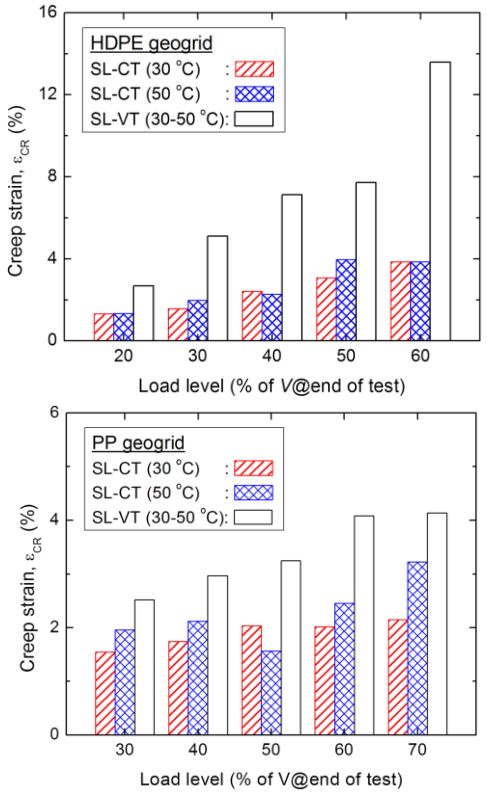

Fig. 9 Comparison of creep strains for: (a) HDPE; and (b) PP

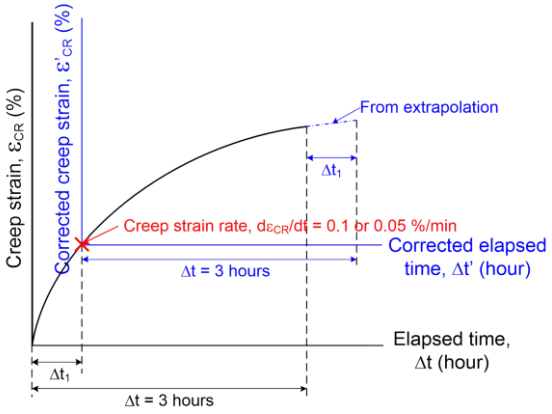

Fig. 10 Creep strain increment for a period of three hours defined for the same initial strain rate

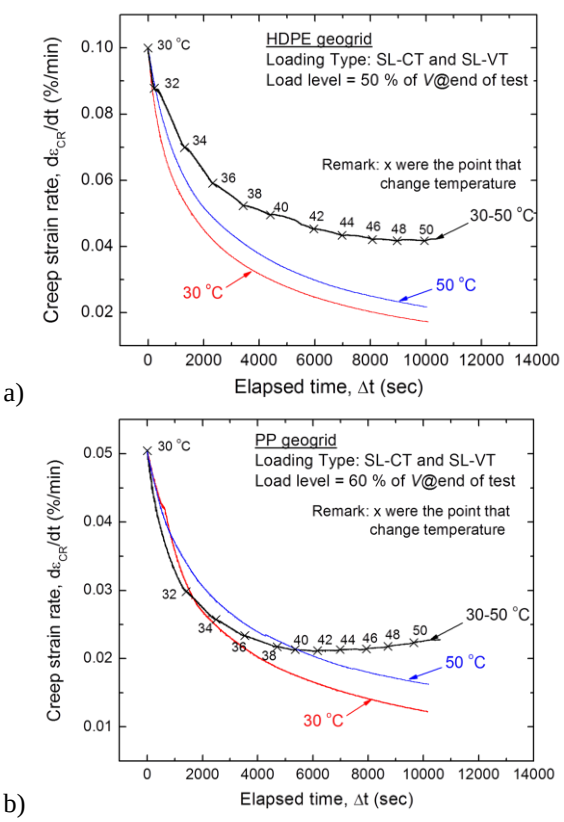

Fig. 11 Creep strain rate vs. time for different test conditions: (a) HDPE; and (b) PP

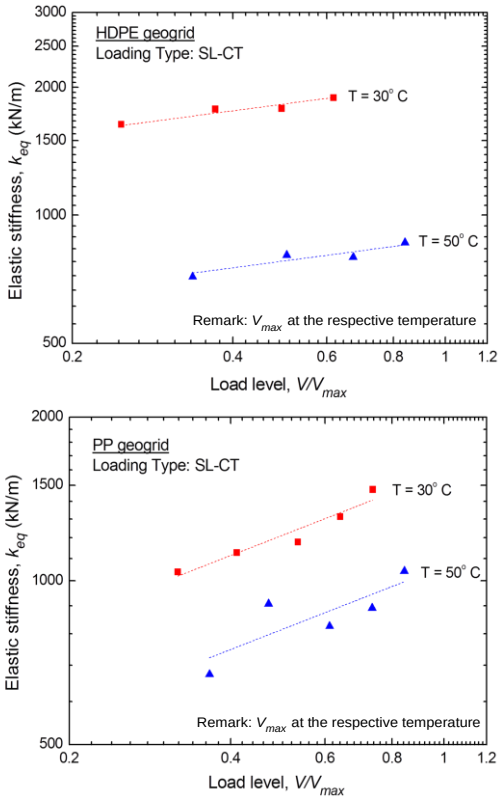

Fig. 12 Elastic stiffness vs. load level: (a) HDPE; and (b) PP

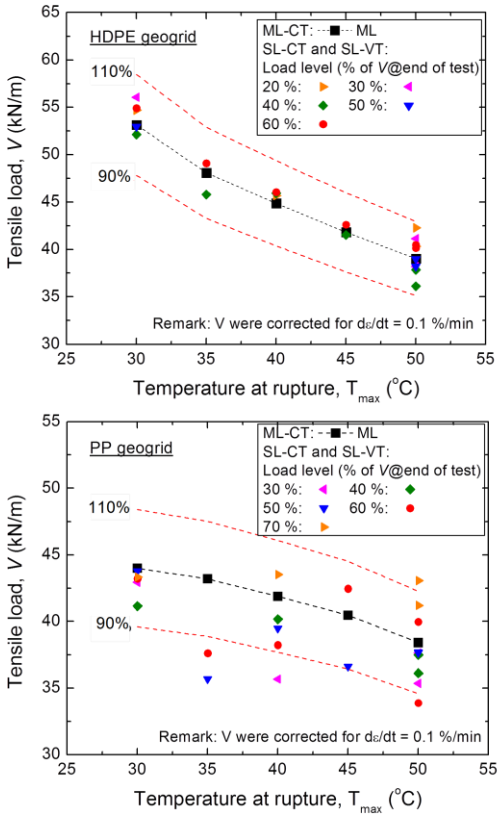

Fig. 13 Residual rupture strength: (a) HDPE; and (b) PP

5. CONCLUSION

The following conclusions with respect to the temperature effects on the load-deformation behaviour of polymer geosynthetics can be derived from the test results presented in this paper:

1. The rupture tensile strength and stiffness of the tested two geogrids decreased while the creep strain increased significantly with an increase in the ambient temperature.
2. The creep strain increment by sustained loading during which the temperature was elevated from 30 °C to 50 °C was significantly larger than the one by sustained loading during otherwise monotonic loading at constant temperature equal to either 30 °C or 50 °C.
3. The residual strengths at the same temperature that were observed in tests with and without pre-rupture sustained loading histories were essentially the same whether the temperature was kept either constant or increasing in the respective tests. This result indicates that the residual strength is essentially a function of temperature at rupture, while creep is not a degrading phenomenon.

6. ACKNOWLEDGEMENTS

The authors are grateful to the National Research Council of Thailand (NRCT), the Commission on Higher Education, the Thailand Research Fund (TRF) and the National Research University (NRU) Project for financial support. Thanks are also extended to Vigor Merger Co., Ltd. and Tencate Geosynthetics (Thailand) Co., Ltd. who provided geogrids for this study.

7. REFERENCES

[1] Koerner RM, Designing with Geosynthetics. New Jersey: Pearson Education, Inc., 2005, ch. 3.

[2] Geosynthetic Institute, "Determination of the Long-Term Design Strength of Stiff Geogrids", GRI Standard Practice GG4(a), 2012.

[3] Geosynthetic Institute, "Determination of the Long-Term Design Strength of Flexible Geogrids ", GRI Standard Practice GG4(b), 2012.

[4] Thornton JS, Paulson JN, and Sandri D, "Conventional and Stepped Isothermal Methods for characterizing long term creep strength of polyester geogrids", in Proc. 6th Int. Conf. on Geosynthetics, 1998, pp. 691-698.

[5] Jeon HY, Kim SH, and Yoo HK, "Assessment of long-term performances of polymer geogrids by accelerated creep test", J. of Polymer Testing, Vol. 21, Aug. 2002, pp. 489-495.

[6] Bueno BS, Costanzi MA, and Zornberg JG, "Conventional and accelerated creep tests on nonwoven needle-punched geotextiles", J. of Geosynthetics International, Vol. 12, Nov. 2005, pp. 276-287.

[7] Jones CJFP and Clarke D, "The residual strength of geosynthetic reinforcement subjected to accelerated creep testing and simulated seismic events", J. of Geotextiles and Geomembranes, Vol. 25, Feb. 2007, pp. 155-169.

[8] França FAN and Bueno BS, "Creep behaviour of geosynthetics using confined accelerated tests", J. of Geosynthetics International, Vol. 18, Oct. 2011, pp. 242-254.

[9] Kongkitkul W, Hirakawa D, Tatsuoka F, and Uchimura T, "Viscous deformation of geosynthetic reinforcement under cyclic loading conditions and its model simulation", J. of Geosynthetics International, Vol. 11, Apr. 2004, pp. 73-99.

[10] Kongkitkul W, Tabsombut W, Jaturapitakkul C, and Tatsuoka F, "Effects of temperature on the rupture strength and elastic stiffness of geogrids", J. of Geosynthetics International, Vol. 19, Apr. 2012, pp. 106-123.

[11] Hirakawa D, Kongkitkul W, Tatsuoka F, and Uchimura T, "Time-dependent stress-strain behaviour due to viscous properties of geogrid reinforcement",J. of Geosynthetics International, Vol. 10, Dec. 2003, pp. 176-199.

[12] Tatsuoka F, Benedetto D, Kongkitkul W, Kongsukpraserat L, Nishi T and Sano Y, "Modelling of ageing on the elasto-viscoplastic behaviour of geomaterial", J. of Soils and Foundations, Vol. 48, Apr. 2008, pp. 155-174.

[13] Kongkitkul W and Tatsuoka F, "A theoretical framework to analyse the behaviour of polymer geosynthetic reinforcement in temperature-accelerated creep tests", J. of Geosynthetics International, Vol. 14, Feb. 2007, pp. 23-38.

[14] Zornberg JG, Byler BB, and Knudsen JW, "Creep of geotextiles using Time-Temperature Superposition methods", J. of ASCE, Vol. 130, Nov. 2004, pp. 1158-1168.

International Journal of GEOMATE, May, 2016, Vol. 10, Issue 21, pp. 1869-1876
MS No. 5192 received on June 19, 2015 and reviewed under GEOMATE publication policies.

Corresponding Author: Thitapan Chantachot